Upwind Relaxation Algorithms for the Navier-Stokes Equations

James L. Thomas*
NASA Langley Research Center, Hampton, Virginia
and
Robert W. Walters†
Virginia Polytechnic Institute & State University, Blacksburg, Virginia

The development of upwind relaxation algorithms for obtaining efficient steady-state solutions to the compressible Navier-Stokes equations is described. The method is second-order accurate spatially and naturally dissipative, using third-order flux splitting of the pressure and convective terms and second-order central differencing for shear and heat flux terms. A line Gauss-Seidel relaxation approach, shown to be unconditionally stable for model convection and diffusion equations, is used. The algorithm is demonstrated for the problem of shock-induced separation over a flat plate.

Introduction

THE purpose of the present paper is to develop an efficient algorithm for obtaining steady-state solutions to the compressible Navier-Stokes equations. Much progress has been made in computational fluid dynamics over the past 15 years toward the development of algorithms for such flows. However, even with the current rapid advance in the speed and available storage of computers, there is a need for improved algorithms to enable viscous flow computations to be used routinely in engineering practice.

Two widely used algorithms are the implicit, approximately factored approach of Beam and Warming[1] and the explicit-implicit approach of MacCormack.[2] In both of these methods, dissipative terms are added for numerical stability, but they are generally difficult to determine optimally. Recently, there has been considerable progress in the development of upwind methods, which recognize the hyperbolic nature of the time-dependent inviscid equations in the construction of naturally dissipative schemes. The improvement in physical treatment comes generally at the expense of increased computational work in comparison to central difference approximations. However, improved algorithms tailored to the properties of the upwind discretization are being developed. The diagonally dominant properties of coefficient matrices arising from such discretizations allow efficient relaxation procedures to be developed, which can increase the overall convergence rate and, thus, offset the increased computational work per time step.[3-6]

An efficient relaxation algorithm for the Navier-Stokes equations is obtained by using upwind differencing for the convective and pressure terms and central differencing for the viscous shear and heat flux terms. The upwind differencing in the present work is implemented using the flux splitting method developed by Van Leer and his co-workers[7,8] including third-order accurate spatial differencing, although the techniques described could be applied to most upwind difference methods. The algorithm is similar in many respects to that of Chakravarthy et al.[9] and Lombard et al.,[10] in that the upwind differencing for the pressure and convective terms is being exploited to obtain efficient solution methods for viscous equations.

The algorithm as applied to the compressible Navier-Stokes equations is described below. Truncation error analysis of the spatial differencing and stability analysis of the relaxation algorithm are given. Computations are made for a series of flows using the thin-layer form of the equations. The effect of grid refinement in the computation of shock-induced boundary-layer separation is also studied.

Governing Equations

The time-dependent compressible Navier-Stokes equations express the conservation of mass, momentum, and energy for an ideal gas in the absence of external forces. The nondimensional form of the equations in conservation law form and

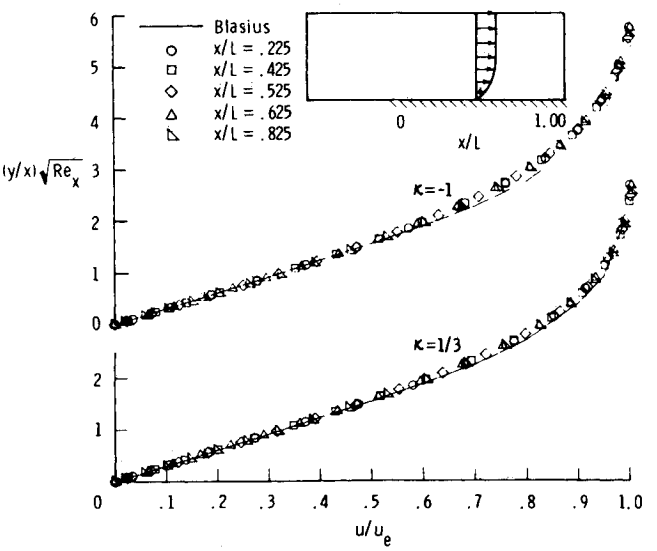

Fig. 1 Comparison of computed velocity distributions with incompressible Blasius solution ($M_\infty = 0.5$, $Re_L = 10{,}000$).

Received June 17, 1985; presented as Paper 85-1501 at the AIAA 7th Computational Fluid Dynamics Conference, Cincinnati, OH, July 15-17, 1985; revision received Aug. 26, 1986.

*Senior Research Scientist, Analytical Methods Branch, Low-Speed Aerodynamics Division. Member AIAA.

†Associate Professor, Aerospace and Ocean Engineering Department. Member AIAA.

Cartesian coordinates is given below

$$\frac{\partial Q}{\partial t}+\frac{\partial F}{\partial x}+\frac{\partial G}{\partial y}=\frac{1}{Re}\left[\frac{\partial R}{\partial x}+\frac{\partial S}{\partial y}\right] \tag{1}$$

where

$$Q=\begin{bmatrix}\rho\\ \rho u\\ \rho v\\ e\end{bmatrix},\ F=\begin{bmatrix}\rho u\\ \rho uu+p\\ \rho uv\\ (e+p)u\end{bmatrix},\ G=\begin{bmatrix}\rho v\\ \rho vu\\ \rho vv+p\\ (e+p)v\end{bmatrix}$$

$$R=\begin{bmatrix}0\\ \tau_{xx}\\ \tau_{xy}\\ r_4\end{bmatrix},\ S=\begin{bmatrix}0\\ \tau_{xy}\\ \tau_{yy}\\ s_4\end{bmatrix}$$

$$\tau_{xx}=2\mu\frac{\partial u}{\partial x}+\lambda\theta,\ \tau_{yy}=2\mu\frac{\partial v}{\partial y}+\lambda\theta$$

$$\tau_{xy}=\mu\left(\frac{\partial u}{\partial y}+\frac{\partial v}{\partial x}\right),\ \theta=\frac{\partial u}{\partial x}+\frac{\partial v}{\partial y}$$

$$r_4=u\tau_{xx}+v\tau_{xy}+\frac{\mu}{Pr}\frac{1}{(\gamma-1)}\frac{\partial a^2}{\partial x}$$

$$s_4=u\tau_{xy}+v\tau_{yy}+\frac{\mu}{Pr}\frac{1}{(\gamma-1)}\frac{\partial a^2}{\partial y}$$

Nondimensionalization of the above equations is with respect to density ρ and speed of sound a. The velocities are u, v, w, and e is the total energy per unit volume. The molecular viscosity μ is determined by the Sutherland law and Stokes hypothesis is used for the bulk viscosity $\lambda=-2\mu/3$. The Reynolds and Prandtl numbers are denoted as Re and Pr. Finally, the pressure p is determined by the ideal-gas law

$$p=(\gamma-1)\left[e-\rho(u^2+v^2)/2\right]$$

where γ is the ratio of specific heats, taken as $\gamma=1.4$.

The thin-layer form of the equations neglect any streamwise diffusion terms and is used below, although the relaxation algorithm considered is applicable to the full equations. The thin-layer form is chosen because it is generally not feasible to resolve the viscous terms in both directions with today's computers, where the general constraint for resolution corresponds to a cell Reynolds number of two. Only the viscous terms normal to the wall are resolved in the thin-layer form and, implemented in generalized coordinates, it has been demonstrated to be applicable to a wide class of problems.

It is straightforward to transform the equations to generalized coordinates of the type $\xi=\xi(x,y)$ and $\eta=\eta(x,y)$. The method discussed below has been implemented in generalized coordinates of this type, although the solutions shown below revert to simple stretching transformation of the type $\xi=\xi(x)$ and $\eta=\eta(y)$.

Spatial Differencing

The governing equations are viewed as composed of inviscid (convective and pressure) and viscous (diffusive) terms. The spatial differencing reflects the predominant nature of the equations in the limit as $Re\to\infty$ (hyperbolic) and $Re\to 0$ (parabolic), i.e., upwind differencing for the convective and pressure terms and central differencing for the shear stress and heat flux terms. The approach represents a natural extension to an upwind flux-vector splitting method recently applied to the analysis of inviscid flow over airfoils in generalized coordinates.[8] Other recent work combining upwind and central differences according to the physics in the limiting Re form of the equations includes that of Coakley,[11] Chakravarthy et al.,[9] and Lombard et al.[10]

The upwind differencing for the convective and pressure terms is based on the flux splitting method developed by Van Leer.[7] These split fluxes have the advantage of first derivative continuity at eigenvalue sign changes, corresponding to sonic and stagnation points, and can represent normal shocks with at most two, and generally one, transition zones. Both second- and third-order spatial differencing schemes have been developed and applied;[8] the improved accuracy with the third-order scheme for viscous flows is evident in the results below.

The inviscid fluxes F and G are split into $F^{\pm}$ and $G^{\pm}$ according to the eigenvalues of the Jacobian matrices $\partial F/\partial Q$ and $\partial G/\partial Q$ and differenced accordingly, as

$$\frac{\partial F}{\partial x}+\frac{\partial G}{\partial y}=\frac{1}{\Delta x}\left[\delta_x^- F^+ +\delta_x^+ F^-\right]+\frac{1}{\Delta y}\left[\delta_y^- G^+ +\delta_y^+ G^-\right] \tag{2}$$

where δ_x^-, δ_y^- denote the backward difference operators and δ_x^+, δ_y^+ the forward difference operators. The split flux differences are represented as a flux balance across a cell, for example,

$$\delta_x^- F^+ +\delta_x^+ F^- =\left[F^+(Q^-)+F^-(Q^+)\right]_{j+1/2}-\left[F^+(Q^-)+F^-(Q^+)\right]_{j-1/2} \tag{3}$$

The notation $F^+(Q^-)$ denotes F^+ evaluated at Q^- and $Q^{\pm}$ represents upwind interpolations to cell interfaces

$$Q_{j\pm 1/2}^{\mp}=Q_j\pm 1/4\left[(1\mp\kappa_x)\nabla_x+(1\pm\kappa_x)\Delta_x\right]Q_j \tag{4}$$

where $Q_{j,k}^n$ denotes cell centered quantities $Q(x,y,t)$, $x=j\Delta x$, $y=k\Delta y$, $t=n\Delta t$, and wherever the script notation would be simply i, j, or n, it is most often dropped. The cell interface location between cells j and $j+1$ is denoted as $j+1/2$. The upwind discretization above corresponds to an interpolation of Q to cell interfaces followed by splitting rather than differencing the split fluxes at cell centers, corresponding to a more local splitting and leading to improved results.[8] The parameter κ determines the accuracy of the spatial differencing: $\kappa=-1$ corresponds to a fully upwind scheme, $\kappa=+1$ to a central difference scheme, and $\kappa=1/3$ to the third-order upwind-biased scheme. The implementation of the method in generalized coordinates in two and three dimensions is given elsewhere.[8,12]

In general, some form of flux limiting is required for the scheme to avoid oscillations at discontinuities in the solution, such as shock waves. The limiting can be implemented by locally modifying the difference quotients in the interpolation of Eq. (4) through comparison with nearby gradients in order to ensure monotone interpolation. The fully upwind scheme has the rather surprising but useful feature that transonic normal shocks can be captured with no overshoots or undershoots with no limiting, which has been used to advantage here and elsewhere.[8,12,13]

The differencing for the viscous terms corresponds to second-order central differences, consistent with the diffusive nature of the shear and heat flux terms. The second derivatives are treated conservatively as differences across cell interfaces of first derivative terms, i.e.,

$$\frac{\partial S}{\partial y}=\frac{1}{\Delta y}\left[S_{j+1/2}-S_{j-1/2}\right]=\frac{1}{\Delta y^2}\left[\mu_{j+1/2}(T_{j+1}-T_j)-\mu_{j-1/2}(T_j-T_{j-1})\right] \tag{5}$$

where the thin-layer approximation to S has been used and

$$T=\begin{bmatrix} 0 \\ u \\ 4v/3 \\ u^2/2+2v^2/3+a^2/[(\gamma-1)Pr] \end{bmatrix}$$

In the extension to generalized coordinates, the overall approach is the same; first derivative terms at cell interfaces are determined through chain rule differentiation. This approach requires a value for the cell volume at a cell interface, which is determined by averaging nearby values. An alternate approach is to evaluate the first derivative terms through Green's theorem, as used by Swanson and Turkel[14] and Chakravarthy et al.,[9] which also requires an averaging process for metric terms at cell interfaces. The principal advantage of the finite-volume form, that of satisfying the difference equations exactly for freestream flow in general curvilinear coordinates, is retained in both formulations.

For the analysis of the truncation error associated with the present scheme, consider the scalar convection-diffusion equation,

$$c\frac{\partial u}{\partial x}-\nu\frac{\partial^2 u}{\partial x^2}=0, \qquad c>0$$

The convection term is approximated with the one-parameter family of higher-order upwind differences as

$$\frac{\delta u}{\delta x}=\frac{1}{4\Delta x}\left[(1-\kappa)u_{j-2}-(5-3\kappa)u_{j-1}+(3-3\kappa)u_j+(1+\kappa)u_{j+1}\right]$$

and the diffusion term with central differences as

$$\frac{\delta^2 u}{\delta x^2}=\frac{1}{\Delta x^2}\left[u_{j+1}-2u_j+u_{j-1}\right]$$

Substitution of the derivative approximations into the convection-diffusion equation and using Taylor series expansions leads to the modified equation,

$$c\frac{\delta u}{\delta x}-\nu\frac{\delta^2 u}{\delta x^2}=c\frac{\partial u}{\partial x}-\nu\frac{\partial^2 u}{\partial x^2}+\frac{\Delta x^2}{12}\left[c(3\kappa-1)\frac{\partial^3 u}{\partial x^3}+\nu\frac{\partial^4 u}{\partial x^4}\right]+\frac{\Delta x^3}{8}c(1-\kappa)\frac{\partial^4 u}{\partial x^4}+O(\Delta x^4)$$

The main consequence of the upwind differencing is the addition of third-order dissipation to the second-order dissipative term arising from the diffusion term. The upwind dissipative term is largest with fully upwind differencing ($\kappa=-1$), but remains of third order. No additional damping is provided with central differencing $\kappa=+1$ and such schemes are susceptible to parasitic odd-even point decoupling. In most present-day central difference codes, third-order fourth-difference terms analogous to those obtained with upwind differencing are explicitly added to damp high-frequency oscillations. The above truncation error analysis differs from the analysis of Reklis and Thomas,[15] who suggest that the upwind dissipation may be orders of magnitude larger than the explicitly added third-order dissipation of central difference codes. First-order upwind differencing leads to first-order second-difference dissipation, which can swamp the discretization of the viscous terms. The higher-order upwind differencing used here overcomes this difficulty and allows viscous flows to be computed accurately.

In general, the scheme is second-order accurate, regardless of the value of κ. The leading-order term arising from convection is dispersive and is, of course, zero for third-order upwind-biased differencing ($\kappa=1/3$). Of the common upwind differencing schemes, the third-order scheme has less dispersion and dissipation than either the fully upwind ($\kappa=-1$) or Fromm's ($\kappa=0$) scheme.

The diffusion term could be differenced with five-point fourth-order discretizations, in which case the accuracy of the combined scheme would be third-order accurate with $\kappa=1/3$. The upwind differencing molecule, in general, spans five points in any one direction so that fourth-order differencing of the viscous terms could be implemented with little additional computational effort, although all of the present results are limited to second order.

Relaxation Algorithm

The relaxation algorithm used in the present work is developed from the backward-time integration scheme applied to Eq. (1)

$$\frac{\Delta Q}{\Delta t}=R^{n+1} \qquad \Delta Q\equiv Q^{n+1}-Q^n \tag{6}$$

where R^{n+1} is the steady-state residual evaluated at time level $n+1$ for the thin-layer equations,

$$R=-\frac{\delta F}{\delta x}-\frac{\delta G}{\delta y}+\frac{1}{Re}\frac{\delta S}{\delta y} \tag{7}$$

Linearizing the residual about the known time level and neglecting the variation of viscosity in the linearization, Eq. (6) can be written as

$$\left[\frac{I}{\Delta t}+\frac{1}{\Delta x}\left(\delta_x^- A^+ + \delta_x^+ A^-\right)+\frac{1}{\Delta y}\left(\delta_y^- B^+ + \delta_y^+ B^-\right)-\frac{1}{Re}\frac{1}{\Delta y^2}\delta_y\left(\mu\delta_y H\right)\right]\Delta Q=R \tag{8}$$

where $A^{\pm}$, $B^{\pm}$, and H are Jacobian matrices of $F^{\pm}$, $G^{\pm}$, and T. The direct solution of the above equation represents a Newton method in the limit as $\Delta t\to\infty$, but requires the inversion of a large banded block matrix equation. The matrix equation is generally approximated for numerical solution. For example, the equations can be approximately factored, leading to block tridiagonal inversions.

Line Gauss-Seidel (LGS) relaxation is applied to Eq. (8) in the present work and is motivated by the form of the coefficient matrix arising from upwind differencing of the convective and pressure terms. The coefficient matrix representing Eq. (8) can be written as

$$\bar{D}\Delta Q_{k-2}+\bar{A}\Delta Q_{k-1}+\bar{B}\Delta Q+\bar{C}\Delta Q_{k+1}+\bar{E}\Delta Q_{k+2}+\bar{H}\Delta Q_{j-2}+\bar{F}\Delta Q_{j-1}+\bar{G}\Delta Q_{j+1}+\bar{I}\Delta Q_{j+2}=R \tag{9}$$

where the coefficients $\bar{A}-\bar{I}$ are 4×4 block matrices and are given in the Appendix. The matrices A^+, B^+ and A^-, B^- are constructed to be non-negative and nonpositive, respectively, through the eigenvalue decomposition used in the flux splitting method. By neglecting the spatial variation of the Jacobian matrices, it is easy to verify from the Appendix that with first-order upwind differencing, the coefficient matrix is diagonally dominant for any time step. Similarly, it is easy to verify that with central differencing ($\kappa=+1$), the only diagonal contributions to the coefficient matrix come from Δt and the viscous terms. With higher-order differencing, the coefficient matrix for inviscid flows at large steps is not diagonally dominant. The ratio of the diagonal element magnitude to the

sum of the off-diagonal element magnitudes goes as

$$3(1-\kappa)/[4+3(1-\kappa)]$$

for κ in the range of -1 to $+1$. Thus, the coefficient matrix is never diagonally dominant for higher-order differencing, but is better conditioned as $\kappa \to -1$. The diagonal dominance criterion is only a sufficient condition for convergence of the linear system. The Von Neumann analysis presented in the next section is relied on for the stability analysis of relaxation applied to Eq. (9).

Many strategies for relaxing the above equation are possible. An essential element in the development of effective strategies is the recognition of the wave propagation in the inviscid field. For example, for streamwise supersonic flows, the Jacobian matrix A^- is zero, representing an upstream propagating influence, and, with a fully upwind scheme in the streamwise direction ($\kappa_x = -1$), the block matrices $\bar{G}$ and $\bar{I}$ are zero, so that a space-marching scheme can be constructed. With line relaxation, quadratic convergence for inviscid supersonic flows is possible,[13] since the relaxation algorithm as $\Delta t \to \infty$ represents direct inversion of the unfactored coefficient matrix.

A second element is the recognition of the stiffness arising in the equations from the small mesh spacing near walls required to resolve viscous effects at high Reynolds numbers. This difficulty is removed in the present method by sweeping in the direction tangent to the wall and accounting for the thin-layer viscous terms implicitly by block line inversions. Alternating the direction of the implicit line inversions is expected to be beneficial for application of the method to general viscous flows and has been also found to be beneficial in inviscid flows with highly stretched grids.

The higher-order differencing of the convective and pressure terms leads to a block pentadiagonal matrix equation to be solved at each line. The work required to solve a block pentadiagonal matrix is identical to that required to solve block periodic tridiagonal matrices, encountered routinely in solutions with approximately factored methods. It is possible to mix the spatial discretizations on the implicit and explicit sides of the equations to reduce the computational work, i.e., first-order differencing on the left-hand side leads only to block tridiagonal matrix equations. It is also possible to use relaxation with upwind differencing on the left side of Eq. (8) and central differencing of the steady-state residual, as demonstrated recently by Napolitano and Walters.[16] Consistent approximations on the explicit and implicit side of the equations lead to faster convergence rates and have been used herein.

The relaxation algorithm is implemented by sweeping back and forth across the mesh, as dictated by stability considerations. The left-to-right sweep can be written as

$$(\bar{D}, \bar{A}, \bar{B}, \bar{C}, \bar{E})\,\Delta Q = R - \bar{F}\Delta Q_{j-1} - \bar{H}\Delta Q_{j-2} \quad (10)$$

and the right-to-left sweep as

$$(\bar{D}, \bar{A}, \bar{B}, \bar{C}, \bar{E})\,\Delta Q = R - \bar{G}\Delta Q_{j+1} - \bar{I}\Delta Q_{j+2} \quad (11)$$

where the notation on the left side of the above two equations represents the pentadiagonal line inversions in the y direction. The solution is updated at the end of each sweep. The algorithm is implemented in delta form so that the solution at convergence is independent of the time step. The boundary conditions, which are discussed subsequently, are linearized using the delta form and incorporated into the matrix of Eq. (9), which leads to increased coupling of the boundary conditions and increased rates of convergence.

The above relaxation algorithm leads to rapid convergence to the steady state for the flows considered below and has proved to be much less sensitive to the time step than approximate factorization methods, since maximal damping occurs for large time steps. The principal disadvantage of the scheme is that it is not completely vectorizable on current vector processors, such as the CDC Cyber 205, due to the recursive nature of the line inversions, as in Eqs. (10) and (11). That is not to say that the computational rate cannot be improved with vector processing, since the line inversions involve only roughly 30% of the total computation. Assuming a factor of 10 for vector-to-scalar computation, a factor of 3 improvement can easily be attained. By realizing that the lower-upper (LU) decomposition of the line inversions can be computed simultaneously for all the lines before beginning the relaxation sweeps implied by Eqs. (10) and (11), further improvements are possible. Most of the work in the inversion occurs in the LU decomposition for 4×4 block line inversions and thus most of the computations can be vectorized. Additionally, Van Leer and Mulder[3] have observed that the coefficient matrices can be frozen for a substantial number of iterations, corresponding to a technique often used in finding the roots of nonlinear equations and effectively reducing the total work in the inversions to essentially that of the forward-backward substitutions. The scalar computational rate on the Cyber 205 at Langley Research Center for the above algorithm is 4×10^{-4} s per grid point per sweep, which can be improved by a factor of 10 by utilizing vector computations and the Jacobian treatment described above.

Stability Analysis

The stability of the present algorithm is investigated by studying model equations of the hyperbolic and parabolic type, thus considering separately the inviscid and viscous terms. The inviscid equation considered is

$$\frac{\partial u}{\partial t} + \lambda_1 \frac{\partial u}{\partial x} + \lambda_2 \frac{\partial u}{\partial y} = 0 \quad (12)$$

where $\lambda_1, \lambda_2 > 0$. The stability analysis for line relaxation is given for $\kappa = 0$ in Ref. 3 and for variable κ in Ref. 12. The analysis accounts approximately for eigenvalues of mixed sign in the full system of conservation equations by relaxation in the same direction and against the wave directions implied by λ_1 and λ_2 in the scalar equation. The main conclusions of the analysis are summarized below.

For first-order differencing, the algorithm is unconditionally stable, regardless of the sweep direction, effectively treating waves moving opposite to the sweep direction at a Courant number less than or equal to unity. For higher-order differencing, it is necessary to alternate the direction of the sweeps in order to construct an unconditionally stable scheme, since relaxation with higher-order treatment of the waves adverse to the sweep direction is unstable. The maximum damping occurs at large time steps for the relaxation, in contrast to approximate factorization methods where an optimal Courant number on the order of 10 in the inviscid field exists for maximum damping.

Consistent approximations on the left and right sides of the unfactored equation lead to the best convergence. With first-order differencing on the left, relaxation is possible, but underrelaxation is required for certain ranges of κ, in particular for $\kappa = -1$ and $\kappa = +1$. Maximum damping for the scheme always occurs with underrelaxation.

The scalar model equation considered for viscous flows is

$$\frac{\partial u}{\partial t} = a\frac{\partial^2 u}{\partial x^2} + b\frac{\partial^2 u}{\partial x \partial y} + c\frac{\partial^2 u}{\partial y^2} \quad (13)$$

where the inequalities

$$a, c > 0,\ b^2 < 4ac \quad (14)$$

ensure that the equation is parabolic. The backward Euler implicit time integration scheme in delta form applied to Eq. (13) results in

$$\left[1 - r\left(a\delta_{xx} + b\delta_{xy} + c\delta_{yy}\right)\right]\Delta u = r\left(a\delta_{xx} + b\delta_{xy} + c\delta_{yy}\right)u \tag{15}$$

where

$$r = \frac{\Delta t}{h^2},\quad h = \Delta x = \Delta y,\quad \Delta u = u^{n+1} - u^n$$

The second derivative terms are defined with a conventional three-point second-order centered difference

$$\delta_{xx}u = u_{j+1} - 2u_j + u_{j-1}$$

$$\delta_{yy}u = u_{k+1} - 2u_k + u_{k-1}$$

Following Mitchell and Griffiths,[17] the cross-derivative term can be differenced either symmetrically or asymmetrically with second-order differences as

$$\delta_{xy}u = \alpha^+\left(\bar{\delta}_{xy}u_{j+1/2,k+1/2} + \bar{\delta}_{xy}u_{j-1/2,k-1/2}\right) + \alpha^-\left(\bar{\delta}_{xy}u_{j-1/2,k+1/2} + \bar{\delta}_{xy}u_{j+1/2,k-1/2}\right) \tag{16}$$

where

$$\bar{\delta}_{xy}u_{j+1/2,k+1/2} = u_{j+1,k+1} - u_{j,k+1} + u_{j,k} - u_{j+1,k}$$

and for consistency

$$\alpha^+ + \alpha^- = 1/2$$

The symmetric treatment of the cross-derivative term corresponds to $\alpha^+ = \alpha^- = 1/4$. The symmetric treatment causes a loss of diagonal dominance for the coefficient matrix resulting from the unfactored equation (15) in comparison to the case of zero cross derivative ($b = 0$). However, Von Neumann analysis of the unfactored equation results in the amplification factor

$$g = \frac{1}{1 + r\psi} \le 1,\ r > 0$$

where ψ is defined in terms of the two spatial frequencies (θ, γ) of the Von Neumann analysis

$$\psi = 2a(1 - \cos\theta) + 2c(1 - \cos\gamma) + b\sin\theta\sin\gamma$$

It can be shown that $\psi > 0$ with the restrictions of Eq. (15), demonstrating the method to be unconditionally stable.[18] The unfactored equation is, of course, not generally practical to solve and relaxation of the unfactored equation is presented subsequently.

The asymmetric treatment of the cross-derivative term is designed to retain diagonal dominance of the matrix resulting from the unfactored equation (15). The coefficients are

$$\alpha^+ = 1/2,\quad \alpha^- = 0,\qquad b > 0$$

$$\alpha^+ = 0,\quad \alpha^- = 1/2,\qquad b < 0$$

and the necessary condition for diagonal dominance is that

$$|b| \le \min(2a, 2c) \tag{17}$$

Application of the Von Neumann analysis to the unfactored equation shows the restriction of Eq. (17) to be both necessary and sufficient for unconditional stability. Since the resulting matrix equation is diagonally dominant, convergence with the asymmetric treatment can be expected to be better than that with the symmetric treatment when the restriction of Eq. (17) holds. The asymmetric treatment has been used with notable success by O'Carroll[19] for the potential equation on skewed meshes and was also used by Chakravarthy et al.[9] for solutions to the Navier-Stokes equations.

Stability of vertical line relaxation applied to the unfactored equation is considered below. With symmetric treatment of the cross-derivative term, the differences can be written in terms of conventional forward (Δ) and backward (∇) differences as

$$\delta_{xx}u = (\Delta_x - \nabla_x)u$$

$$\delta_{xy}u = 1/4\left[(\nabla_x + \Delta_x)(\nabla_y + \Delta_y)\right]u$$

The relaxation matrix corresponding to a left-to-right sweep across the mesh is easily constructed by replacing the forward difference operator Δ_x with -1 on the left side of the unfactored equation, as

$$\left\{1 - r\left[-a(1 + \nabla_x) + (b/4)(\nabla_x - 1)(\nabla_y + \Delta_y) + c\delta_{yy}\right]\right\}\Delta u = r\left(a\delta_{xx} + b\delta_{xy} + c\delta_{yy}\right)u \tag{18}$$

The relaxation matrix corresponding to a right-to-left sweep is similarly constructed by replacing the backward difference ∇_x on the left-hand side with $+1$. Applying Von Neumann analysis to Eq. (18) results in the complex amplification factor

$$g = \frac{\bar{a} + i\bar{b}}{\bar{c} + i\bar{d}}$$

where

$$\bar{a} = 1 + r(2a\cos\theta - b\sin\theta\sin\gamma)/2$$

$$\bar{b} = \bar{d} = r(2a\sin\theta - b\cos\theta\sin\gamma)/2$$

$$\bar{c} = r\psi + \bar{a}$$

and ψ is as defined above. Since the imaginary parts of both numerator and denominator of g are equal, it is sufficient for stability that

$$\bar{c}^2 - \bar{a}^2 = r\psi(r\psi + 2\bar{a}) > 0$$

which is always satisfied since $r\psi > 0$ and

$$r\psi + 2\bar{a} = 2[1 + ra + 2cr(1 - \cos\gamma)] \ge 0$$

The stability for the right-to-left sweep is identical to that above. Thus, line relaxation applied to the model problem is unconditionally stable with symmetric treatment of the cross-derivative term.

Maximum damping for the relaxation scheme occurs for large time steps, $r \to \infty$, in analogy with upwind relaxation for the inviscid equations. It is known that for large time steps, the convergence of the above line Gauss-Seidel relaxation behaves as $-\ell n\rho \alpha h^2$, where ρ is the spectral radius. The convergence can be substantially improved by applying overrelaxation, for which, with optimum overrelaxation, $-\ell n\rho\alpha h$. Thus, for flows with significant viscous stresses in both directions, overrelaxation of the viscous terms is expected to increase convergence rates substantially. Note that with thin-layer equations and the sweeping direction tangential to the wall, the viscous terms are all treated fully implicitly.

Computational Results

The first model problem considered is flow over a flat plate. Results are shown in Fig. 1 for a freestream Mach number

M_∞ of 0.5 and a Reynolds number Re_L, based on freestream velocity and the length of the plate, of 10,000. The computational domain is sketched and extends half a length upstream of the leading edge. Inflow conditions of constant entropy and total pressure and zero vertical velocity were applied upstream of the plate; outflow conditions corresponding to specified pressure were applied along the top and rear of the domain. No-slip, adiabatic wall conditions were specified on the plate with symmetry conditions ahead of the plate. The results were obtained on a 31×41 grid, uniform in the x direction and stretched in the y direction.

The computational results shown for $\kappa = -1$ and $1/3$ indicate that both upwind discretizations resolve the boundary layer reasonably well with approximately 20 points in the layer. The increased accuracy obtained with the third-order differencing is evident in these and other calculations. With first-order upwind differencing, in contrast, the boundary-layer thickness is four to five times that shown.

The second model problem is that of an oblique shock impinging on a laminar boundary layer developing on a flat plate. The model problem corresponds to the experiments of Hakkinen et al.[20] at a freestream Mach number of 2.0 and a Reynolds number based on freestream velocity and the length from the leading edge of the plate to the shock impingement point of 2.96×10^5. The shock is of sufficient strength to cause a separation of the developing laminar boundary layer. Several results are available in the literature for comparison,[1,21] even though none are believed to be of sufficient resolution to be judged nominally exact.

The computational grid is shown in Fig. 2; a sketch of the physical processes in the interaction is shown, indicating the initial compression due to the separating boundary layer, the expansion over the separation bubble, and the final recompression wave due to the turning at the wall. The boundary conditions were as follows. At the supersonic inflow, all variables were specified; at cell centers below the impinging shock location, freestream was specified and, at cell centers above the impinging shock, variables obtained from the jump conditions across the shock were specified. Along the top of the domain, the boundary conditions were overspecified and the variables were specified from the shock jump conditions. At the wall, no-slip adiabatic wall conditions were imposed. Since the flow at the rear of the computational domain is an outflow boundary and predominantly supersonic, extrapolation of all variables from the interior was used.

Computational results from a grid refinement study are shown in Fig. 3, using fully upwind differencing in the streamwise direction and third-order upwind-biased differencing in the vertical direction. The initial mesh density corresponded to that described in Ref. 1 with the exception that the domain was extended vertically so that the leading-edge shock passed through the downstream outflow boundary. Mesh densities two and three times the initial mesh density were used. The initial mesh density is too coarse to adequately define the pressure plateau or the skin friction. As shown in Fig. 3, details of the separated flow region are generally resolved with the second mesh, although a small difference exists between the second and third meshes near reattachment. Outside of the separated flow region, very little difference exists in the results from any of the meshes. The detail accorded in the present calculations shows clearly the pressure plateau in the separation zone. Pressure contours, shown in Fig. 4, clearly define the compression and expansion waves in the interaction region.

Comparisons of the present computations with experiment and other computations are shown in Fig. 5. All of the computations were done with a mesh equally spaced in the streamwise direction and stretched in the vertical direction. The results of MacCormack and Baldwin were taken from Ref. 21; the results of Beam and Warming were made with the code described in Ref. 1, but on the mesh shown in Fig. 2. There is generally close agreement between all of the results

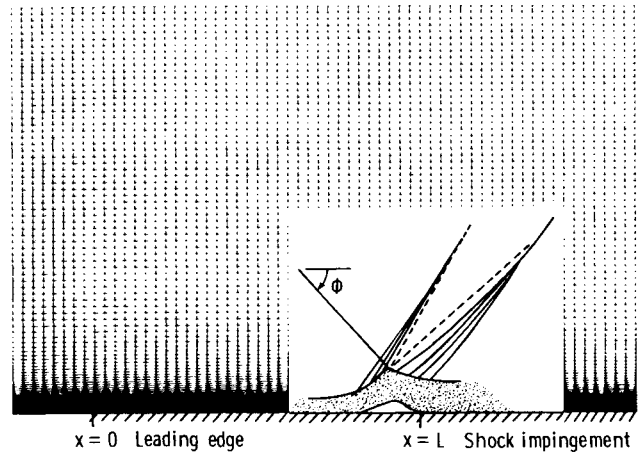

Fig. 2 Computational grid for shock/boundary-layer interaction ($Re_L = 2.96 \times 10^5$, $M_\infty = 2.0$, $\phi = 32.6$, 61×113 grid).

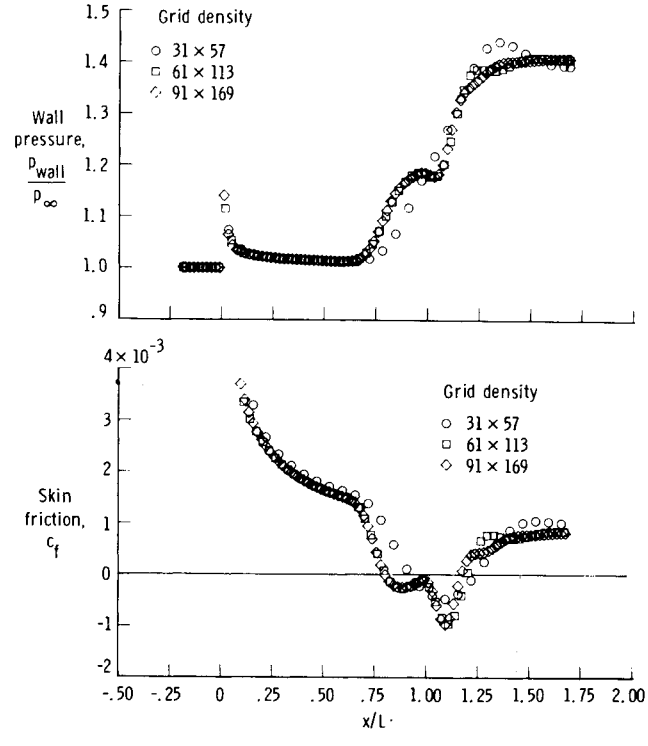

Fig. 3 Grid refinement for shock/boundary-layer interaction.

and the experiment, although there are noticeable differences in the levels of skin friction in the separated zone. Unfortunately, skin-friction measurements in the separation zone were not possible; the solid symbols in the figure denote locations where the presence of separated flow was identified. The computations with the present method were with the thin-layer assumption, while the others were with the complete Navier-Stokes equations. However, the spacing in the streamwise direction is not sufficient to adequately resolve the viscous terms in that direction, so it is not surprising that the thin-layer results agree closely with the other results, even for this separated boundary-layer flow.

The computations for each of the three meshes were made with a local Courant number of 10^3 and initialized with freestream conditions in the interior of the domain. On the coarse mesh, the L_2 norm of the residual was driven to machine zero (10^{-12}) in 150 iterations with $\kappa_x = -1$, $\kappa_y = 1/3$ and less than 125 iterations with $\kappa_x = \kappa_y = -1$. One iteration is defined here as two sweeps across the mesh, consistent with

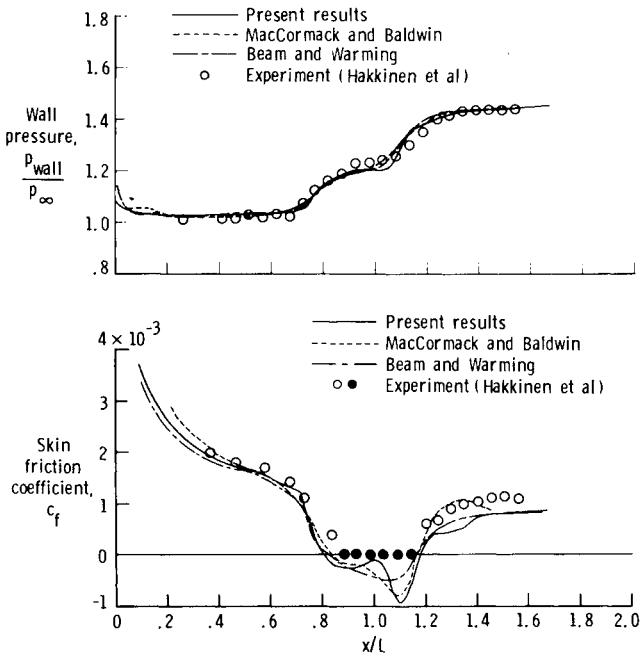

Fig. 4 Pressure contours for shock/boundary-layer interaction.

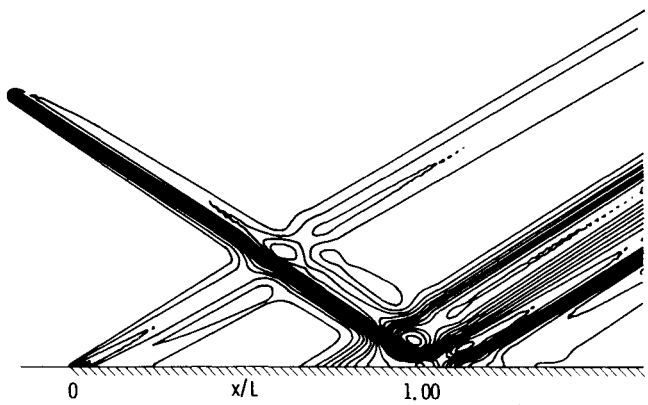

Fig. 5 Comparison of computations with experiment for shock/boundary-layer interactions.

the number of sweeps across the mesh used in the approximate factorization method. On the finest mesh, the L_2 norm of the residual was reduced more than 4 orders of magnitude in 150 iterations. The integral of the wall pressure on the plate was monitored during the iteration and can be taken as a measure of global convergence of the physical solution; the pressure integral converged to its asymptotic value on the 3 meshes in 50, 75, and 100 iterations, respectively.

Conclusions

An efficient algorithm for steady-state solutions to the compressible Navier-Stokes equations has been described. The algorithm is cast in conservation law form and is naturally dissipative, using third-order flux splitting for the pressure and convective terms and second-order central differencing for diffusion terms. The improvement with the third-order differencing in comparison to second-order for viscous flows is apparent from truncation error analysis and the computations presented. A line Gauss-Seidel relaxation approach is used to obtain rapid convergence; the relaxation is shown to be unconditionally stable for model convection and diffusion equations. The method is much less sensitive to the time step than current approximate factorization methods. Maximum damping occurs at large time steps so that large Courant numbers are advantageous for convergence and the method is formulated so that the steady-state solution is independent of the time step. Applications of the method have been made using the thin-layer assumptions for a series of model problems, including shock-induced boundary-layer separation. The physical solutions of the method compare closely with experiment and other available analytical and numerical methods.

Appendix

The 4×4 block matrices forming the coefficient matrix of Eq. (9) are given below.

$$\bar{D} = \frac{1}{\Delta y}\left[-\alpha_y B^+_{k-1/2}\right]$$

$$\bar{A} = \frac{1}{\Delta y}\left[-\beta_y B^+_{k-1/2} + \alpha_y B^+_{k+1/2} - \gamma_y B^-_{k-1/2}\right] - \frac{1}{Re\Delta y^2}\left[\mu_{k-1/2} H_{k-1}\right]$$

$$\bar{B} = \frac{1}{\Delta x}\left[\beta_x\left(A^+_{j+1/2} - A^-_{j-1/2}\right) - \gamma_x A^+_{j-1/2} + \gamma_x A^-_{j+1/2}\right] + \frac{1}{\Delta y}\left[\beta_y\left(B^+_{k+1/2} - B^-_{k-1/2}\right) - \gamma_y B^+_{k-1/2} + \gamma_y B^-_{k+1/2}\right] - \frac{1}{Re\Delta y^2}\left[-\left(\mu_{k+1/2} + \mu_{k-1/2}\right) H_k\right] + \frac{1}{\Delta t}$$

$$\bar{C} = \frac{1}{\Delta y}\left[\gamma_y B^+_{k+1/2} - \alpha_y B^-_{k-1/2} + \beta_y B^-_{k+1/2}\right] - \frac{1}{Re\Delta y^2}\left[\mu_{k+1/2} H_{k+1}\right]$$

$$\bar{E} = \frac{1}{\Delta y}\left[\alpha_y B^-_{k+1/2}\right]$$

$$\bar{H} = \frac{1}{\Delta x}\left[-\alpha_x A^+_{j-1/2}\right]$$

$$\bar{F} = \frac{1}{\Delta x}\left[-\beta_x A^+_{j-1/2} + \alpha_x A^+_{j+1/2} - \gamma_x A^-_{j-1/2}\right]$$

$$\bar{G} = \frac{1}{\Delta x}\left[\gamma_x A^+_{j+1/2} - \alpha_x A^-_{j-1/2} + \beta_x A^-_{j+1/2}\right]$$

$$\bar{I} = \frac{1}{\Delta x}\left[\alpha_x A^-_{j+1/2}\right]$$

where

$$\alpha_x = -\frac{\phi}{4}(1-\kappa_x), \qquad \beta_x = 1 - \frac{\phi}{2}\kappa_x$$

$$\gamma_x = \frac{\phi}{4}(1+\kappa_x)$$

and similarly for α_y, β_y, and γ_y in terms of κ_y. The parameter ϕ is zero for first-order differencing and one otherwise. With the finite-volume formulation, Jacobians for the inviscid terms are evaluated at cell interface locations and those for viscous terms are evaluated at cell center locations.

Acknowledgments

The authors express their appreciation to Jerry C. South Jr. of NASA Langley Research Center for many informative discussions of the present method.

References

[1] Beam, R.M. and Warming, R.F., "An Implicit Factored Scheme for the Compressible Navier-Stokes Equations," *AIAA Journal*, Vol. 16, April 1978, pp. 393–402.

[2] MacCormack, R.W., "A Numerical Method for Solving the Equations of Compressible Viscous Flow," *AIAA Journal*, Vol. 20, Sept. 1982, pp. 1275–1281.

[3]Van Leer, B. and Mulder, W.A., "Relaxation Methods for Hyperbolic Equations," Delft Univ. of Technology, Delft, The Netherlands, Rept. 84-20, 1984.

[4]Chakravarthy, S.R., "Relaxation Methods for Unfactored Implicit Schemes," AIAA Paper 84-0165, Jan. 1984.

[5]Lombard, C.K., Venkatapathy, E., and Bardina, J., "Universal Single Level Implicit Algorithm for Gasdynamics," AIAA Paper 84-1533, June 1984.

[6]Rai, M.M., "A Relaxation Approach to Patched-Grid Calculations with the Euler Equations," AIAA Paper 85-0295, Jan. 1985.

[7]Van Leer, B., "Flux-Vector Splitting for the Euler Equations," ICASE Rept. 82-30, Sept. 1982 (also, *Lecture Notes in Physics*, Vol. 170, 1982, pp. 507–512).

[8]Anderson, W.K., Thomas, J.L., and Van Leer, B., "A Comparison of Finite Volume Flux Vector Splittings for the Euler Equations," AIAA Paper 85-0122, Jan. 1985.

[9]Chakravarthy, S.R., Szema, K-Y., Goldberg, U.C., Gorski, J.J., and Osher, S., "Application of a New Class of High Accuracy TVD Schemes to the Navier-Stokes Equations," AIAA Paper 85-0165, Jan. 1985.

[10]Lombard, C.K., Bardina, J., Venkatapathy, E., and Oliger, J., "Multi-dimensional Formulation of CSCM—An Upwind Flux Difference Eigenvector Split Method for the Compressible Navier-Stokes Equations," AIAA Paper 83-1895, July 1983.

[11]Coakley, T.J., "Implicit Upwind Methods for the Compressible Navier-Stokes Equations," AIAA Paper 83-1958, July 1983.

[12]Thomas, J.L., Van Leer, B., and Walters, R.W., "Implicit Flux-Split Schemes for the Euler Equations," AIAA Paper 85-1680, July 1985.

[13]Walters, R.W. and Dwoyer, D.L., "An Efficient Iteration Strategy Based on Upwind/Relaxation Schemes for the Euler Equations," AIAA Paper 85-1529, July 1985.

[14]Swanson, R.C. and Turkel, E., "A Multistage Time-Stepping Scheme for the Navier-Stokes Equations," AIAA Paper 85-0035, Jan. 1985.

[15]Reklis, R.P. and Thomas, P.D., "Shock-Capturing Algorithm for the Navier-Stokes Equations," *AIAA Journal*, Vol. 20, Sept. 1982, pp. 1212–1218.

[16]Napolitano, M. and Walters, R.W., "An Incremental Line Gauss-Seidel Method for the Incompressible and Compressible Navier-Stokes Equations," AIAA Paper 85-0033, Jan. 1985.

[17]Mitchell, A.R. and Griffiths, D.F., *The Finite Difference Method in Partial Differential Equations*, Wiley, New York, 1980, pp. 125–129.

[18]Richtmyer, R.D. and Morton, K.W., *Difference Methods for Initial-Value Problems*, Interscience Publishers, New York, 1967, pp. 206–208.

[19]O'Carroll, M.J., "Diagonal Dominance and S.O.R. Performance with Skew Nets," *International Journal for Numerical Methods in Engineering*, Vol. 10, 1976, pp. 225–240.

[20]Hakkinen, R.J., Greber, I., Trilling, L., and Arbarbanel, S.S., "The Interaction of an Oblique Shock Wave with a Laminar Boundary Layer," NASA Memo-2-18-59W, March 1959.

[21]MacCormack, R.W. and Baldwin, B.S., "A Numerical Method for Solving the Navier-Stokes Equations with Application to Shock-Boundary Layer Interactions," AIAA Paper 75-1, Jan. 1975.